Generation of magnonic frequency combs via a two-tone microwave drive

Zeng-Xing Liu,[1,*] Jiao Peng,[1,2] and Hao Xiong[3]

[1]*School of Electronic Engineering & Intelligentization, Dongguan University of Technology, Dongguan, Guangdong 523808, China*
[2]*School of Information and Optoelectronic Science and Engineering, South China Normal University, Guangzhou, Guangdong 510006, China*
[3]*School of Physics, Huazhong University of Science and Technology, Wuhan 430074, China*

(Received 2 January 2023; revised 15 February 2023; accepted 1 May 2023; published 12 May 2023)

Magnonic frequency combs, a direct analog of optical frequency combs in the field of spin waves, have recently received considerable attentions due to their potential applications in high-precision magnonic frequency metrology. However, due to the weak nonlinear interaction of magnons, it is difficult to generate a wide-bandwidth magnonic frequency comb under a low power drive. Here, we present an efficient mechanism for the generation of a wide-bandwidth magnonic frequency comb via a two-tone microwave driving in a magnomechanical system. Numerical simulations show that the magnetostrictive effect can be greatly enhanced by the beat frequency signal from the two-tone microwave driving field, and a robust magnonic frequency comb can be observed at low power. Furthermore, abundant nonperturbative features appear in the magnonic spectrum, implying that the magnons as bosons may also be similar to photons in atom-molecular systems. Our scheme thus provides a pathway for the generation of a flat magnonic frequency comb under a low-power driving condition that may be beneficial for precision metrology based on magnonic platforms as well as the understanding of nonlinear magnomechanic dynamics.

DOI: 10.1103/PhysRevA.107.053708

I. INTRODUCTION

The magnetostrictive effect describing the phenomenon that magnetic materials will stretch or shorten in the magnetization direction in response to an external magnetic field was first discovered in the 19th century by Joule [1] and has since been the subject of extensive research that has made great progress in sensor technology [2,3]. Among all magnetic material systems, the cavity magnomechanical system based on the magnetic insulator yttrium iron garnet (YIG) sphere stands out owing to its excellent material and geometrical properties [4], which provides a powerful platform for coherent coupling between magnons and phonons [5–10]. Many intriguing phenomena have been reported in cavity magnomechanics, ranging from magnomechanically induced transparency or absorption [5], magnon-photon-phonon entanglement [11–13], and magnon squeezing [14,15] to the magnetostrictive-force-induced slow-light effect [16–18] and the mechanical bistability in a Kerr-modified cavity magnomechanical system [6]. Moreover, the magnetostrictive effect is essentially a nonlinear interaction that will cause the nonlinear oscillation of the magnons excited in the YIG sphere [7,19] and then produce the Stokes and anti-Stokes frequency sidebands similar to those in atomic-molecular systems [20–22].

Magnonic frequency combs, a kind of frequency spectrum with discrete and equally spaced spectral lines generated in the microwave (gigahertz) frequency range, attracted particular attention in spintronics in the context of understanding the nonlinear interaction based on magnonic [23–28]. Microwave frequency comb generation due to a $\chi^{(3)}$ nonlinearity in sapphire introduced by a dilute concentration of paramagnetic Fe^{3+} spins has been reported [29,30]. More recently, several methods to generate magnonic frequency combs have been proposed. For example, magnonic frequency combs generated in a ferromagnetic thin film based on nonlinear magnon-skyrmion interaction were theoretically studied [23]. Also, spin-wave frequency combs through the nonlinear four-magnon scattering in a microstructured waveguide were experimentally demonstrated [24]. Moreover, magnonic frequency combs via the resonantly enhanced magnetostrictive effect were theoretically proposed [25] and the optomagnonic frequency combs based on Brillouin light scattering were also envisaged [26], as well as other relevant studies [31–35]. In addition, similar to the way the optical frequency comb revolutionized the precision timing and high-resolution spectroscopy [36,37], the extension of the frequency comb concept to the field of spin waves is expected to bring new innovations to the high-precision magnonic frequency metrology and spectroscopy, which, in particular, brings an important application prospect for the precise measurement of complex magnonic spatiotemporal dynamics [7]. However, due to the restrictions of engineering and material technology, the nonlinear magnonic interaction realized in experiments is still very weak, and it is difficult to generate a wide-bandwidth magnonic frequency comb, particularly under a low power condition, which limits their practical applications to a large extent. Therefore, how to generate a wide-bandwidth magnonic frequency comb at low power driving is still a pivotal and challenging problem.

To this aim, we propose an efficient mechanism for the generation of a wide-bandwidth magnonic frequency comb via a two-tone microwave driving in a magnomechanical

*liuzx@dgut.edu.cn

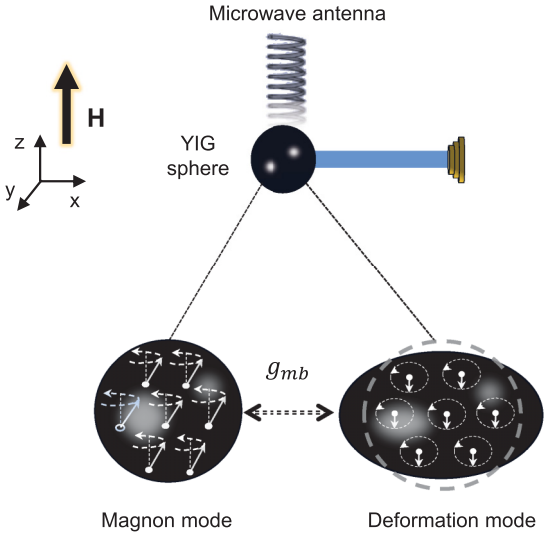

FIG. 1. Schematic illustration of a magnomechanical system, in which the YIG sphere is directly driven via a local microwave antenna to excite the magnon mode. A uniform magnetic field (H) is applied along the z direction to saturate the magnetization. The dynamic magnetization of the magnon causes the deformation of the YIG sphere, which gives rise to the magnomechanical interaction between the magnon mode and the vibrational mode and g_{mb} is the coupling strength.

system. We find that the use of a two-tone microwave driving to generate magnonic frequency combs, compared to the previous scheme [23,24], has its inherent advantages in, for instance, low power conditions, flat frequency comb teeth, and abundant nonperturbation features. In physics, a beat frequency signal from the two-tone microwave driving field can extremely enhance the nonlinear magnetostrictive interaction between the mechanical mode and the Kittel mode of the YIG sphere, inducing the generation of a robust magnonic frequency comb even at low power driving. Furthermore, abundant nonperturbation signals are found in the magnonic spectrum, which is similar to the high-order harmonic generation in atom-molecular systems [20–22], suggesting that magnons as bosons may also exhibit phenomena that are similar to those in atomic-molecular systems. In addition to providing an effective way to enhance the magnetostrictive effect, our results provide an alternative for the development of the magnonic frequency comb in the field of spin waves and may find potential applications in precision metrology based on spintronic platforms [36–39].

II. PHYSICAL MODEL AND THEORY

The physical model we consider is a magnomechanical system, as is schematically shown in Fig. 1, in which a highly polished ferromagnetic insulator YIG sphere is directly driven via a local microwave antenna. A uniform bias magnetic field with the strength H is introduced along the z direction and a uniform magnon mode (Kittel mode) of the YIG sphere will be excited. The frequency of the Kittel mode is determined by the external bias magnetic field, i.e., $\omega_m = \varrho H$, where $\varrho/2\pi = 28$ GHz/T is the gyromagnetic ratio [4]. The Hamiltonian of the Kittel mode, in quantum mechanical language, can be described in the form $H_m = \hbar\omega_m \hat{m}^\dagger \hat{m}$ via the Holstein-Primakoff transformations [40], where $\hbar$ is the reduced Planck's constant, $\hat{m} = \sqrt{\frac{V_m}{2\hbar\varrho M_s}}(M_x - iM_y)$ is the boson annihilation operator of the Kittel mode, with V_m the YIG sphere volume, M_s the saturation magnetization, and $M_{x,y,z}$ the magnetization components. Experiment has shown that the varying magnetization induced by the magnon excitation will cause the deformation of the geometric shape of the YIG sphere, introducing mechanical degrees of freedom in the YIG crystal [5]. In turn, the deformation of the YIG sphere also affects the magnetization. As a consequence, the deformation mode in the YIG sphere could be used as the mechanical mode that couples to the magnon mode through magnetostrictive forces [5–7]. The magnetostrictive interaction between the magnon mode and the mechanical mode can be described by a radiation pressure-like Hamiltonian [41], i.e., $H_{\rm int} = \hbar g_{mb} \hat{m}^\dagger \hat{m}(\hat{b}^\dagger + \hat{b})$, where $\hat{b}(\hat{b}^\dagger)$ is the boson annihilation (creation) operator of the mechanical mode and g_{mb} the single magnon-phonon coupling strength. For a 250-μm-diameter YIG sphere, the magnon-phonon coupling strength can be achieved $g_{mb} = 2\pi \times 9.88$ mHz in experiment [5]. It should be point out that the magnon-phonon coupling strength is proportional to $1/D^2$ with D being the YIG sphere diameter, which indicates that smaller YIG spheres are favorable for stronger magnon-phonon coupling. However, due to the limitation of material technology, the volume of the YIG sphere is difficult to further reduce, and thus it is particularly important to find another way to enhance the nonlinear interaction between magnons and phonons [42].

In the present work, we assume that the Kittel mode in the YIG sphere is excited by a two-tone microwave driving field, one of which has the Rabi frequency $\Omega_0 = \sqrt{5N_{\rm spin}}\varrho B_0/4$ and the other has the Rabi frequency $\Omega_d = \sqrt{5N_{\rm spin}}\varrho B_d/4$ with $B_{0(d)}$ the driving magnetic field, $\omega_{0(d)}$ the driving frequency, and $N_{\rm spin}$ the total number of the spins in the YIG sphere. The microwave driving power can be calculated via $P_{0(d)} = \frac{B_{0(d)}^2}{2\mu_0} Ac$, where u_0 is vacuum magnetic permeability, $A = \pi(D/2)^2$ is the cross-sectional area, and c is the speed of an electromagnetic wave propagating through the vacuum [11]. To simplify the description, we refer to the two-tone microwave driving field, respectively, as the microwave pumping and probe fields although the power of the microwave probe field may exceed the power of the pumping field. Under the low-lying excitations, i.e., the excited magnon number is much smaller than the total spin number $\langle m^\dagger m\rangle/2N_{\rm spin} \ll 1$, the time-dependent Hamiltonian of the two-tone microwave driving field can be described as $H_d = i\hbar\Omega_0(\hat{m}^\dagger e^{-i\omega_0 t} + \hat{m}e^{i\omega_0 t}) + i\hbar\Omega_d(\hat{m}^\dagger e^{-i\omega_d t} + \hat{m}e^{i\omega_d t})$ [11], where ω_0 and ω_d are the driving frequencies of the microwave pumping and probe fields, respectively. To make the pumping term time independent, a frame rotating at the frequency ω_0 of the pumping field is adopted, i.e., a unitary transformation $\mathbf{U}(t) = \exp(-i\omega_0 \hat{m}^\dagger \hat{m} t)$ is applied. The Hamiltonian of the system, therefore, can be written as

$$\begin{aligned} \mathrm{H} &= \mathbf{U}(t) H \mathbf{U}^\dagger(t) - i\hbar \mathbf{U}(t) \frac{\partial \mathbf{U}^\dagger(t)}{\partial t} \\ &= \hbar\Delta_m \hat{m}^\dagger \hat{m} + \hbar\omega_b \hat{b}^\dagger \hat{b} + \hbar g_{mb} \hat{m}^\dagger \hat{m}(\hat{b}^\dagger + \hat{b}) \\ &\quad + i\hbar\Omega_0(\hat{m} + \hat{m}^\dagger) + i\hbar\Omega_d(\hat{m}e^{i\Delta_d t} + \hat{m}^\dagger e^{-i\Delta_d t}), \end{aligned} \tag{1}$$

where ω_b is the intrinsic frequency of the mechanical mode. $\Delta_m = \omega_m - \omega_0$ is the detuning from the microwave pumping field and the magnon mode, and $\Delta_d = \omega_d - \omega_0$ is the beat frequency between the microwave pumping and probe fields. Based on the Hamiltonian and introducing the dissipation with the Markov approximation [43], the evolution of the magnon and phonon modes can be described by the Heisenberg-Langevin equations, i.e., $\dot{\hat{o}} = i/\hbar[H, \hat{o}](\hat{o} = \hat{b}, \hat{m})$, and then we can obtain the following equations:

$$\begin{aligned} \dot{m} &= (i\Delta_m - \kappa_m)m - ig_{mb}(b + b^*)m + \Omega_0 + \Omega_d e^{-i\Delta_d t}, \\ \dot{b} &= (-i\omega_b - \kappa_b)b - ig_{mb}m^*m, \end{aligned} \tag{2}$$

where κ_m and κ_b are, respectively, the damping rates of the magnon and phonon modes. In the semiclassical approximation, the operators of the magnon and phonon modes are reduced to their expectation values, viz. $m(t) \equiv \hat{m}(t)$ and $b(t) \equiv \hat{b}(t)$, and the thermal noise terms are dropped safely in the present work. Equations (2) show that the magnon and phonon modes from the same YIG sphere influence each other via the magnetostrictive interaction and the temporal evolution of the magnon and phonon modes in the case of the two-tone microwave driving can be obtained by solving the nonlinear Eqs. (2) under various initial values of m and b. In the present work, the initial condition is chosen as $m|_{t=0} = 0$, $b|_{t=0} = 0$ for convenience, and Eqs. (2) are solved numerically by using the Runge-Kutta method. Further, the frequency spectrum of the magnonic dynamics can be obtained by completing the fast Fourier transform of the time series [26].

III. RESULTS AND DISCUSSION

Figure 2(a) shows a high dependence of the magnonic spectrum on the microwave pumping power P_0 in the case of a two-tone microwave driving. We can see clearly that the number of comb lines increases as the microwave pumping power increases. Importantly, under the current experimental parameters [5], the magnonic frequency comb can be generated even under weak microwave driving, which provides an effective pathway to realize low-power magnonic frequency combs. To be specific, when the power of the microwave pumping field is chosen as $P_0 = 0.05$ mW, (P_d is fixed at 5.86 μW, corresponding to the driving magnetic field $B_d = 0.1 \times 10^{-5}$ T), as shown in Fig. 2(c), visibly, several comb teeth appear in the magnonic spectrum. Furthermore, when the microwave pumping power is increased to $P_0 = 0.5$ mW, as is shown in Fig. 2(b), a robust magnonic frequency comb can be obtained. In our scheme, the beat frequency between the microwave pumping field and the probe field resonates with the mechanical mode of the YIG sphere, viz. $\Delta_d = \omega_b$. In this case, the process of the magnonic frequency comb generation can be understood as the frequency downconversion and upconversion (i.e., Stokes and anti-Stokes) processes. More specifically, the frequency ω of the nth comb tooth can be written as $\omega = \omega_0 \pm n\omega_f$, where ω_0 is the pumping frequency and $\omega_f = \omega_b$ the repetition frequency. Here, it should be pointed out that, in the case of low power driving, it is impossible to generate a magnonic frequency comb by using a monochromatic microwave driving field (i.e., $P_d = 0$) under the same parameter conditions [as shown in Fig. 2(d)], as reported in Ref. [25].

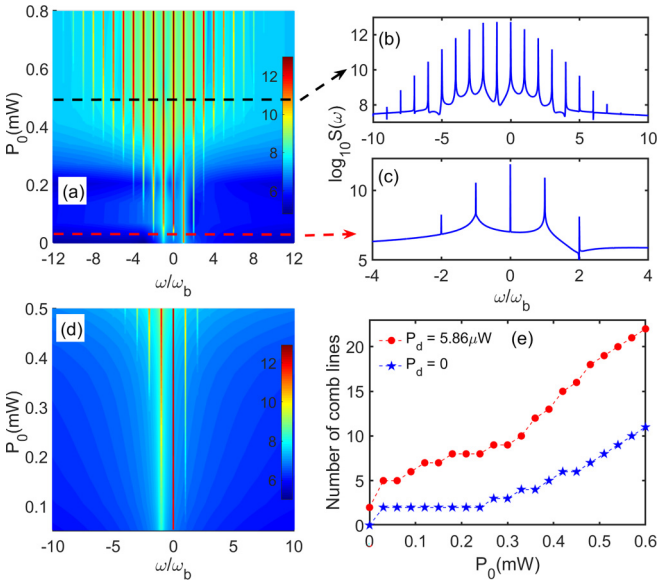

FIG. 2. The contour plot of the magnonic spectrum varies with the pumping power P_0 in the case of (a) two-tone microwave driving (P_d is fixed at 5.86 μW, corresponding to the driving magnetic field $B_d = 0.1 \times 10^{-5}$ T) and (d) monochromatic microwave driving ($P_d = 0$). The color indicates the amplitude of the frequency combs. (b),(c) The magnonic spectra under the different pumping powers $P_0 = 0.5$ mW and $P_0 = 0.05$ mW, respectively. (e) Number of the comb lines as a function of the microwave pumping power P_0 in the case of two-tone microwave driving (red dots) and monochromatic microwave driving (blue stars). The simulation parameters are chosen from the recent experiment [5] $\omega_b/2\pi = 11.42$ MHz, $\kappa_m/2\pi = 0.56$ MHz, $\kappa_b/2\pi = 150$ Hz, $g_{mb}/2\pi = 9.88$ mHz, $\Delta_m = \omega_b$.

Physically, these are two different mechanisms for the generation of magnonic frequency combs in the magnomechanical system. For a magnomechanical system driven by a monochromatic microwave field, the effective beat frequency is achieved by the interaction between the microwave driving and the excited magnon mode, and then magnonic frequency combs are generated by the phonon laser action induced by the resonantly enhanced magnetostrictive effect [25], whereas, the phonon excitation requires a higher threshold power. Numerical calculations show that, under the recent experimental parameters, magnonic frequency combs can emerge only when the driving magnetic field exceeds about $B_0 = 0.75 \times 10^{-5}$ T (corresponding to the driving power $P_0 = 0.33$ mW) [25], which greatly limits their application at low power. To break this bottleneck, a scheme for magnonic frequency combs' generation by using a two-tone microwave driving is proposed, i.e., a microwave probe field is applied. Under the circumstances, by adjusting the beat frequency between the microwave pumping field and the probe field to make it directly resonant with the mechanical mode of the YIG sphere, the magnetostrictive effect will be extremely enhanced, thus greatly reducing the driving field power required to induce the generation of magnonic frequency combs. For comparison,

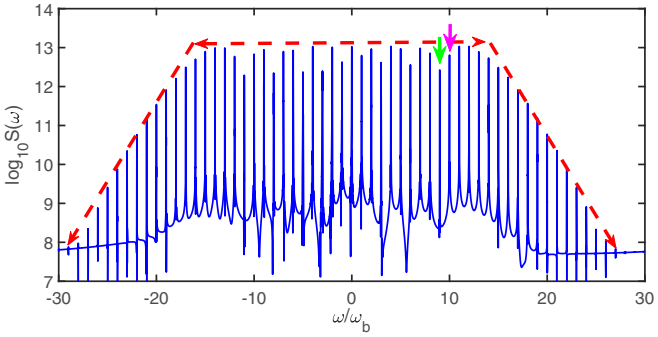

FIG. 3. The wide-bandwidth magnonic spectrum under the microwave pumping power $P_0 = 7.5$ mW (corresponding to the driving magnetic field $B_d = 3.5 \times 10^{-5}$ T) and $B_d = 10B_0$. The other parameters are the same as those in Fig. 2.

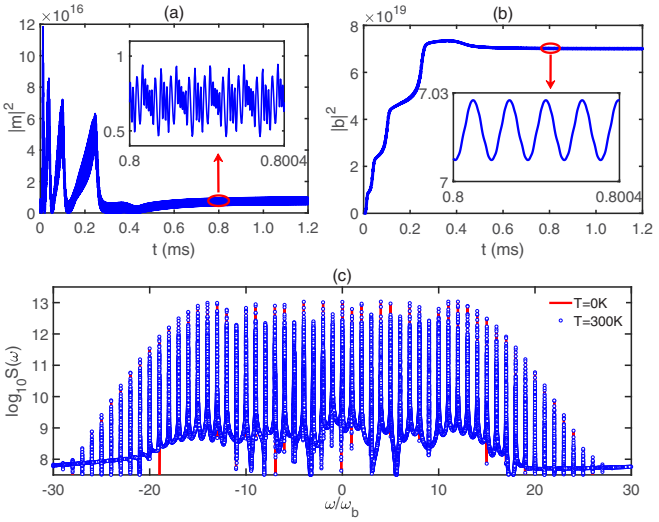

FIG. 4. (a),(b) Time evolution of the magnon number $|m|^2$ and phonon number $|b|^2$ under the pumping power $P_0 = 7.5$ mW. (c) The magnonic spectra under different temperatures (0 K and 300 K). The other parameters are the same as those in Fig. 2.

the number of comb lines as a function of the microwave pumping power P_0 under two different driving conditions is shown in Fig. 2(e). Obviously, a robust frequency comb can be obtained with a low-power drive in the case of two-tone microwave driving (red dots), which is significantly better than the case where the magnonic frequency comb is seeded by a monochromatic driving field (blue stars) or other methods [23,24].

To obtain a wide-bandwidth magnonic frequency comb, the pumping power is further increased to $P_0 = 7.5$ mW, as shown in Fig. 3. Of note, the magnonic spectrum has been shifted wholly by a microwave pumping frequency ω_0 because the coupling Eqs. (2) were discussed in a frame rotating at frequency ω_0. A typical frequency comb structure similar to that in the field of optics is obtained in the spin waves' domain, in which the magnonic frequency comb has equal frequency intervals. Furthermore, the total comb width is greatly enlarged and the number of comb lines expands to about ∼60. In addition, there is a plateau region in the magnonic spectrum where all the comb teeth have nearly the same intensity (as shown by the horizontal red dotted line) and end up with a sharp cutoff. Meanwhile, we can observe a wealth of nonlinear characteristics in the comb spectrum, especially the typical nonperturbation signal [22,44], for example, the amplitude of the tenth-order comb tooth (pink arrow) is larger than the ninth-order comb tooth (green arrow). In essence, the magnonic frequency combs discussed here are induced by nonlinear magnetostrictive effects, which are quite different from the high-order harmonics generation in intense driven atomic-molecular systems [20–22]. Nevertheless, some of the important nonlinear phenomena appearing in atomic-molecular systems can also be observed in the magnomechanical system as a result of the magnetostrictive effect, such as frequency conversion and nonperturbed features, suggesting that magnons as bosons may also behave like photons.

In what follows, we discuss the influence of temperature on the generation of magnonic frequency combs. Without loss of generality, we assume that the system is coupled to a high-temperature thermal bath and that both the phonon and magnonic modes of the system are driven by the thermal noise [25]. Here, the thermal noises are processed as Gaussian random numbers with average values $m_{\rm th} \approx k_B T/\hbar\omega_m$ for the magnonic mode and $n_{\rm th} \approx (e^{\hbar\omega_b/k_B T} - 1)^{-1} \approx k_B T/\hbar\omega_b$ for the phonon mode, respectively, with k_B the Boltzmann constant and T the ambient temperature [43]. In this case, the magnonic spectrum can be obtained by numerically solving the coupled Eqs. (2) with the addition of thermal noise by using the same method; the result is shown in Fig. 4(c). Visibly, the magnonic spectrum at room temperature ($T = 300$ K) is not very different from that at zero temperature ($T = 0$ K), indicating that the influence of thermal noise on the generation of magnonic frequency combs is negligible. The reason is that the steady-state magnon and phonon numbers are free from the thermal bath. To be specific, the average number of thermal magnons at room temperature can be estimated to be about $m_{\rm th} \sim 10^3$. However, as shown in Fig. 4(a), under the strong two-tone microwave driving, the time evolution of the magnon number $|m|^2$ undergoes a transient process at the beginning and finally stabilizes at about 0.7×10^{16}, which is extremely large compared to the mean number of thermal magnons. In addition, thermal phonons have very little effect on the evolution of the phonon motion. As shown in Fig. 4(b), the time evolution of the phonon number $|b|^2$ undergoes a dramatic growth and finally stabilizes at about 7.02×10^{19}, which is much larger than the mean number of thermal phonons at room temperature ($n_{\rm th} \sim 10^6$). Therefore, the generation of magnonic frequency combs via the two-tone microwave driving proposed here is robust against thermal noise. It should be pointed out that the magnetoelastic coefficient is a temperature-dependent constant, that is, the magnon-phonon coupling strength is influenced by the ambient temperature, thus affecting the generation of magnonic frequency combs [45], which will be treated elsewhere.

The magnetostrictive interaction between magnonic and vibrational modes dynamically modify the properties of the mechanical oscillator, such as the vibrational frequency shift (magnonic spring effect) and an additional damping

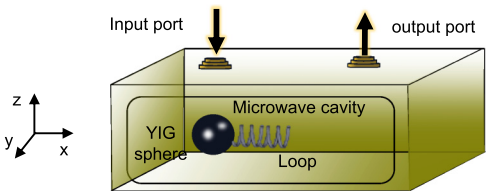

FIG. 5. Schematic diagram of a cavity magnomechanical system for the experimental detection of the produced magnonic frequency combs. A weak microwave probe field enters the microwave cavity through the input port and the other port is used for detection.

rate, which is known as dynamical backaction [7]. The magnetostriction-induced damping rate reads $\gamma_{\rm mag} = \beta|m|^2$, where $\beta = \frac{g_{mb}^2\gamma_m}{4}\{\frac{1}{(\Delta_m+\omega_b)^2+\gamma_m^2} - \frac{1}{(\Delta_m-\omega_b)^2+\gamma_m^2}\}$ can be both negative and positive, depending on the detuning between the microwave pumping field and the magnon mode. In the blue-detuned regime, the total damping rate of the mechanical oscillator $\Gamma_b = \kappa_b + \gamma_{\rm mag}$ (κ_b is the intrinsic vibrational damping rate) can be negative, which results in the amplification of the vibrational motions, also referred to as the phonon laser action. Under this mechanism, the generation of robust magonic frequency combs can be observed [25]. In addition, it was shown that, in the case of a YIG sphere, phonons inevitably couple to other higher-order magnetostatic modes (Walker modes) in addition to the Kittel mode [45–47]. In this case, the magnomechanical damping rate should be modified, phenomenologically, we have [47]

$$\gamma_{\rm mag} = \beta|m|^2 + \alpha|m|^2. \tag{3}$$

Here $\alpha/2\pi \sim$ pHz is the correction factor for the magnomechanical damping rate, resulting from the phonons coupled to other Walker modes. At a rough estimate, α is an order of magnitude from β for the present parameters, i.e., $\alpha/2\pi \sim \beta/2\pi \sim$ pHz, showing that the coupling between the other Walker modes and the mechanical mode is as effective as the Kittel mode. Therefore, from this perspective, the coupling of mechanical mode with other Walker modes will also affect the generation of magnonic frequency combs, which will be an interesting topic and a full-fledged study in this direction requires further analysis.

Finally, it is necessary to discuss the experimental detection of the produced magnonic frequency combs. In the experiment, the magnomechanical system was placed in a three-dimensional microwave cavity (as shown in Fig. 5). Due to the coupling between the magnon and the microwave photon, the spectral information of the magnon can be readout through the photons, as the authors of Refs. [5,6] suggested. More specifically, in the cavity magnomechanical system, the magnon-photon coupling is considered, and their interaction Hamiltonian under the rotating-wave approximation can be written as $H_{am} = \hbar g_{am}(am^\dagger + a^\dagger m)$ [5], where a depicts the cavity photon mode and g_{am} is the magnon-photon coupling strength. In this case, the dynamics of the system satisfy

$$\begin{aligned}
\dot{m} &= (i\Delta_m - \kappa_m)m - ig_{am}a - ig_{mb}(b+b^*)m \\
&\quad + \Omega_0 + \Omega_d e^{-i\Delta_d t}, \\
\dot{b} &= (-i\omega_b - \kappa_b)b - ig_{mb}m^*m, \\
\dot{a} &= (-i\omega_a - \kappa_a)a - ig_{am}m - i\Omega_p e^{-i\omega_p t},
\end{aligned} \tag{4}$$

where ω_a is the frequency of the microwave photon mode with damping rate κ_a. Ω_p is the amplitude of the input microwave probe field whose frequency is ω_p. For a weak microwave probe field, that is, Ω_p is small enough to ensure that $g_{am}a \ll g_{mb}(b+b^*)m$, therefore, Eq. (4) can be decoupled into two sets of equations: one is the same as Eq. (2) that describes the generation of magnonic frequency combs and the another

$$\dot{a} = (-i\omega_a - \kappa_a)a - ig_{am}m - i\Omega_p e^{-i\omega_p t} \tag{5}$$

describes the microwave probe photons scattered by the magnons. Due to the linearity of magnon-photon coupling, there is almost no influence on the generation of magnonic frequency combs. Furthermore, it can be seen from Eq. (5) that the magnon can be regarded as the source of the microwave cavity photon, hence, the spectral information of the magnon can be readout indirectly by connecting a vector network analyzer in the probe port [5,6].

IV. CONCLUSION

In summary, a mechanism for the generation of a wide-bandwidth magnonic frequency comb by using a two-tone microwave driving in a magnomechanical system was theoretically investigated. The underlying mechanism can be understood in terms of the beat frequency from the two-tone microwave driving field greatly enhancing the nonlinear magnetostrictive interaction, inducing a robust magnonic frequency comb even at low power driving. The numerical simulation results showed that the total combwidth of the magnonic frequency comb can be extended to about 60 orders. In addition, a typical complete comb structure (plateau and cutoff) was observed and the nonperturbation characteristics appearing in the magnonic spectrum were discussed in detail. More beneficially, the magnonic frequency comb present here is robust against the thermal noise at room temperature. Beyond their fundamental scientific significance, our scheme offers an idea for realizing a robust magnonic frequency comb in the spin waves' domain and may find potential applications in high-precision frequency metrology based on magnonic devices.

ACKNOWLEDGMENTS

This work was supported by the National Science Foundation (NSF) of China (Grants No. 12105047 and No. 12022507) and the Guangdong Basic and Applied Basic Research Foundation (Grants No. 2022A1515010446 and No. 2020A1515110969).

[1] J. P. Joule, On a new class of magnetic forces, Ann. Electr. Magn. Chem. **8**, 219 (1842).

[2] F. T. Calkins, A. B. Flatau, and M. J. Dapino, Overview of magnetostrictive sensor technology, J. Intell. Mater. Syst. Struct. **18**, 1057 (2007).

[3] F. Narita, Z. Wang, H. Kurita, Z. Li, Y. Shi, Y. Jia, and C. Soutis, A review of piezoelectric and magnetostrictive biosensor materials for detection of COVID-19 and other viruses, Adv. Mater. **33**, 2005448 (2021).

[4] A. A. Serga, A. V. Chumak, and B. Hillebrands, YIG magnonics, J. Phys. D **43**, 264002 (2010).

[5] X. Zhang, C.-L. Zou, L. Jiang, and H. X. Tang, Cavity magnomechanics, Sci. Adv. **2**, e1501286 (2016).

[6] R.-C. Shen, J. Li, Z.-Y. Fan, Y.-P. Wang, and J. Q. You, Mechanical Bistability in Kerr-Modified Cavity Magnomechanics, Phys. Rev. Lett. **129**, 123601 (2022).

[7] C. A. Potts, E. Varga, V. A. S. V. Bittencourt, S. V. Kusminskiy, and J. P. Davis, Dynamical Backaction Magnomechanics, Phys. Rev. X **11**, 031053 (2021).

[8] Z.-X. Liu and H. Xiong, Magnon laser based on Brillouin light scattering, Opt. Lett. **45**, 5452 (2020).

[9] Z. Shen, G.-T. Xu, M. Zhang, Y.-L. Zhang, Y. Wang, C.-Z. Chai, C.-L. Zou, G.-C. Guo, and C.-H. Dong, Coherent Coupling between Phonons, Magnons, and Photons, Phys. Rev. Lett. **129**, 243601 (2022).

[10] D. Hatanaka, M. Asano, H. Okamoto, Y. Kunihashi, H. Sanada, and H. Yamaguchi, On-Chip Coherent Transduction between Magnons and Acoustic Phonons in Cavity Magnomechanics, Phys. Rev. Appl. **17**, 034024 (2022).

[11] J. Li, S.-Y. Zhu, and G. S. Agarwal, Magnon-Photon-Phonon Entanglement in Cavity Magnomechanics, Phys. Rev. Lett. **121**, 203601 (2018).

[12] M. Yu, H. Shen, and J. Li, Magnetostrictively Induced Stationary Entanglement between Two Microwave Fields, Phys. Rev. Lett. **124**, 213604 (2020).

[13] W. Qiu, X. Cheng, A. Chen, Y. Lan, and W. Nie, Controlling quantum coherence and entanglement in cavity magnomechanical systems, Phys. Rev. A **105**, 063718 (2022).

[14] J. Li, Y.-P. Wang, J.-Q. You, and S.-Y. Zhu, Squeezing microwaves by magnetostriction, Natl. Sci. Rev. nwac247 (2022).

[15] W. Zhang, D.-Y. Wang, C.-H. Bai, T. Wang, S. Zhang, and H.-F. Wang, Generation and transfer of squeezed states in a cavity magnomechanical system by two-tone microwave fields, Opt. Express **29**, 11773 (2021).

[16] C. Kong, B. Wang, Z.-X. Liu, H. Xiong, and Y. Wu, Magnetically controllable slow light based on magnetostrictive forces, Opt. Express **27**, 5544 (2019).

[17] T.-X. Lu, H. Zhang, Q. Zhang, and H. Jing, Exceptional-point-engineered cavity magnomechanics, Phys. Rev. A **103**, 063708 (2021).

[18] Z.-X. Liu, B. Wang, C. Kong, H. Xiong, and Y. Wu, Magnetic-field-dependent slow light in strontium atom-cavity system, Appl. Phys. Lett. **112**, 111109 (2018).

[19] S.-N. Huai, Y.-L. Liu, J. Zhang, L. Yang, and Y.-X. Liu, Enhanced sideband responses in a PT-symmetric-like cavity magnomechanical system, Phys. Rev. A **99**, 043803 (2019).

[20] Z. Zhai, Q. Zhu, J. Chen, Z.-C. Yan, P. Fu, and B. Wang, High-order harmonic generation with Rydberg atoms by using an intense few-cycle pulse, Phys. Rev. A **83**, 043409 (2011).

[21] J. P. Marangos, Solid progress, Nat. Phys. **7**, 97 (2011).

[22] P. Huang, X.-T. Xie, X. Lü, J. Li, and X. Yang, Carrier-envelope-phase-dependent effects of high-order harmonic generation in a strongly driven two-level atom, Phys. Rev. A **79**, 043806 (2009).

[23] Z. Wang, H.-Y. Yuan, Y. Cao, Z.-X. Li, R. A. Duine, and P. Yan, Magnonic Frequency Comb Through Nonlinear Magnon-Skyrmion Scattering, Phys. Rev. Lett. **127**, 037202 (2021).

[24] T. Hula, K. Schultheiss, F. J. T. Gonçalves, L. Körber, M. Bejarano, M. Copus, L. Flacke, L. Liensberger, A. Buzdakov, A. Kákay, M. Weiler, R. Camley, J. Fassbender, and H. Schultheiss, Spin-wave frequency combs, Appl. Phys. Lett. **121**, 112404 (2022).

[25] H. Xiong, Magnonic frequency combs based on the resonantly enhanced magnetostrictive effect, Fundamental Res. **3**, 8 (2023).

[26] Z.-X. Liu and Y.-Q. Li, Optomagnonic frequency combs, Photon. Res. **10**, 2786 (2022).

[27] S. Muralidhar, A. A. Awad, A. Alemán, R. Khymyn, M. Dvornik, D. Hanstorp, and J. Åkerman, Sustained coherent spin wave emission using frequency combs, Phys. Rev. B **101**, 224423 (2020).

[28] Z.-X. Liu, H. Xiong, M.-Y. Wu, and Y.-Q. Li, Absorption of magnons in dispersively coupled hybrid quantum systems, Phys. Rev. A **103**, 063702 (2021).

[29] D. L. Creedon, K. Benmessaï, and M. E. Tobar, Frequency Conversion in a High Q-Factor Sapphire Whispering Gallery Mode Resonator due to Paramagnetic Nonlinearity, Phys. Rev. Lett. **109**, 143902 (2012).

[30] D. L. Creedon, K. Benmessaï, W. P. Bowen, and M. E. Tobar, Four-Wave Mixing from Fe^{3+} Spins in Sapphire, Phys. Rev. Lett. **108**, 093902 (2012).

[31] Z.-X. Liu, B. Wang, H. Xiong, and Y. Wu, Magnon-induced high-order sideband generation, Opt. Lett. **43**, 3698 (2018).

[32] Z.-X. Liu, C. You, B. Wang, H. Xiong, and Y. Wu, Phase-mediated magnon chaos-order transition in cavity optomagnonics, Opt. Lett. **44**, 507 (2019).

[33] W.-L. Xu, Y.-P. Gao, C. Cao, T.-J. Wang, and C. Wang, Nanoscatterer-mediated frequency combs in cavity optomagnonics, Phys. Rev. A **102**, 043519 (2020).

[34] Z. W. Zhou, X. G. Wang, Y. Z. Nie, Q. L. Xia, and G. H. Guo, Spin wave frequency comb generated through interaction between propagating spin wave and oscillating domain wall, J. Magn. Magn. Mater. **534**, 168046 (2021).

[35] J. Sun, S. Shi, and J. Wang, Strain Modulation of Magnonic frequency comb by magnon-skyrmion interaction in ferromagnetic materials, Adv. Eng. Mater. **24**, 2101245 (2022).

[36] Th. Udem, R. Holzwarth, and T. W. Hänsch, Optical frequency metrology, Nature (London) **416**, 233 (2002).

[37] S. A. Diddams, K. Vahala, and T. Udem, Optical frequency combs: Coherently uniting the electromagnetic spectrum, Science **369**, eaay3676 (2020).

[38] A. V. Chumak, Vasyuchka, and B. Hillebrands, Magnon spintronics, Nat. Phys. **11**, 453 (2015).

[39] D. Lachance-Quirion, S. P. Wolski, Y. Tabuchi, S. Kono, K. Usami, and Y. Nakamura, Entanglement-based single-shot detection of a single magnon with a superconducting qubit, Science **367**, 425 (2020).

[40] T. Holstein and H. Primakoff, Field dependence of the intrinsic domain magnetization of a ferromagnet, Phys. Rev. **58**, 1098 (1940).

[41] M. Aspelmeyer, T. J. Kippenberg, and F. Marquardt, Cavity optomechanics, Rev. Mod. Phys. **86**, 1391 (2014).

[42] M. Goryachev, W. G. Farr, D. L. Creedon, Y. Fan, M. Kostylev, and M. E. Tobar, High-Cooperativity Cavity QED with Magnons at Microwave Frequencies, Phys. Rev. Appl. **2**, 054002 (2014).

[43] C. W. Gardiner and P. Zoller, *Quantum Noise* (Springer, Berlin, 2000).

[44] H. Xiong, L.-G. Si, X.-Y. Lü, X. Yang, and Y. Wu, Carrier-envelope phase-dependent effect of high-order sideband generation in ultrafast driven optomechanical system, Opt. Lett. **38**, 353 (2013).

[45] V. A. S. V. Bittencourt, C. A. Potts, Y. Huang, J. P. Davis, and S. Viola Kusminskiy, Magnomechanical backaction corrections due to coupling to higher order Walker modes and Kerr nonlinearities, Phys. Rev. B **107**, 144411 (2023).

[46] C. Gonzalez-Ballestero, D. Hümmer, J. Gieseler, and O. Romero-Isart, Theory of quantum acoustomagnonics and acoustomechanics with a micromagnet, Phys. Rev. B **101**, 125404 (2020).

[47] C. A. Potts, Y. Huang, V. A. S. V. Bittencourt, S. Viola Kusminskiy, and J. P. Davis, Dynamical backaction evading magnomechanics, Phys. Rev. B **107**, L140405 (2023).